Soils and Foundations 2013;53(1):64–76

The Japanese Geotechnical Society

Soils and Foundations

www.sciencedirect.com
journal homepage: www.elsevier.com/locate/sandf

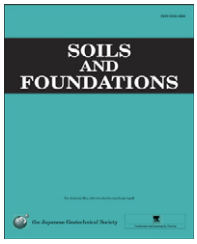

Feasible method, utilizing density changes, for estimating *in situ* dynamic strength and deformation properties of sand samples

Takaharu Shogaki[a,*], Kazuhiro Kaneda[b]

[a]*National Defense Academy, 1-10-20 Hashirimizu, Yokosuka 239-8686, Japan*
[b]*Research and Development Institute, Takenaka Corporation, Otsuka 1-5-1, Inzai, Chiba 270-1395, Japan*

Received 30 September 2011; received in revised form 29 June 2012; accepted 1 September 2012
Available online 16 February 2013

Abstract

Laboratory tests and design reliability are directly controlled by sample quality. The frozen sampling (FS) method is useful for dynamic strength and deformation tests of undisturbed clean sand. However, it is very expensive and requires considerable equipment. The sample quality of Toyoura sands obtained from 48 mm and 75 mm samplers are scrutinized based on void ratio, dynamic strength and deformation properties through model and cyclic undrained triaxial tests. A conventional method for estimating *in-situ* dynamic strength and deformation properties of sand samples utilizing density changes is examined and the applicability of the proposed method is discussed for the samples obtained from Niigata sand deposits.

The main conclusions obtained from this study are summarized as follows:

(1) A conventional method for estimating *in-situ* void ratio (e_0), D_r, stress ratio (R_{L20}) in a 20 cyclic time frame and the initial modulus of rigidity (G_0) of sand samples utilizing density changes is proposed.

(2) The *in-situ* R_{L20} and G_0 estimated from the proposed method for sand samples from tube samplers were similar to those of frozen sampling and the *in-situ* modulus of initial rigidity was calculated from the secondary wave velocity for Niigata sand deposits.

Therefore, dynamic strength and deformation properties changes, caused by sampling, can be modified appropriately to an *in-situ* condition by this proposed method.

Keywords: Dynamic strength; Frozen sampling; Relative density; Rigidity; Sample disturbance; Sand; Stress ratio; Tube sampling; Void ratio; (IGC: C6,D7)

1. Introduction

Laboratory tests and design reliability are directly controlled by sample quality. Studies on the dynamic strength and deformation properties of geotechnical materials have been conducted since the Niigata Earthquake in 1964, and the basis for design code specifications, site investigations and laboratory tests have been established from the results. However, the liquefaction of soils, excluding sand, in the Hanshin Awaji Earthquake of 1995 and the Tohoku-chiho/Taiheiyo-oki Earthquake of 2011, and various other reasons, have made revisions to the design codes necessary. These areas of research have become more important as stronger earthquakes reoccur throughout Japan, particularly with the possibility for earthquake occurrence in the Kanto and Tokai regions. The frozen sample (FS) method for undisturbed clean sand in dynamic strength and deformation tests is useful. However, it is very expensive and requires considerable

*Corresponding author.
E-mail address: shogaki@nda.ac.jp (T. Shogaki).
Peer review under responsibility of The Japanese Geotechnical Society.

Production and hosting by Elsevier

http://dx.doi.org/10.1016/j.sandf.2012.12.004

equipment; and therefore, it is limited to geotechnical investigations of important soils, building structures and research samplings, *etc.* A simpler and more economical sampling method, such as the tube sampling (TS) method, can be used. In order to establish a TS method for natural sand deposits and a technique to evaluate the quality of the sample obtained, systematic samplings were conducted by the Soil Sampling Committee of the Japanese Geotechnical Society (JGS) in 1987 and 1988 and the Japan Geotechnical Consultant Association (JGCA) in 1998. From the JGS-1987 investigation, it was reported that there was a sample recovery ratio (R_r) of only 67% for samplings when using this method.

Shogaki (1997) developed a new sampler called a 45-mm sampler, which has a 45-mm inner diameter and a two-chambered hydraulic piston; its applicability was tested through unconfined compression tests at six different sites in Japan (Shogaki and Sakamoto, 2004) on Pisa clay (Shogaki et al., 2005) and Niigata sand (Shogaki et al., 2001, 2006). Estimation methods (Shogaki, 2006) for the *in situ* undrained shear strength and the correcting consolidation parameters (Shogaki, 1996) of natural deposits for samples obtained from a tube sampler were proposed. However, an economically feasible method for estimating the *in situ* dynamic strength and deformation properties of sand samples obtained from a tube sampler had not been established until now.

In this paper, the sample quality of Toyoura sand obtained from 45-mm and 75-mm samplers is examined based on the void ratio, the dynamic strength and the deformation properties through cyclic undrained triaxial and model tests. An economically feasible method for estimating the *in situ* dynamic strength and deformation properties of sand samples, utilizing changes in density, is proposed and the applicability of the proposed method for samples obtained from Niigata sand deposits is discussed.

2. Soil samples and test procedures

2.1. Grain size distribution properties of samples

Toyoura sand was used for estimating the *in situ* dynamic strength and deformation properties of sand samples. Fig. 1 and Table 1 show the grain size distribution curves and their results for both Toyoura sand and Niigata sand (Shogaki et al., 2006). The soil particle density (ρ_s) of the Toyoura sand is 2.653 g/cm^3. The uniformity coefficient (U_c) and curvature coefficient (U'_c) are 1.5 and 0.94, respectively. The U_c and U'_c values of the Niigata sand are in the range of 1.5～2.2 and 1.0～1.2, respectively. The percentage of the grain size of the Niigata sand, that is smaller than 0.075 mm, is 0.6～6.8%. Therefore, both types of sand have similar grain size properties.

Cyclic triaxial tests on the reconstituted sand are performed according to the standards of the Japanese Geotechnical Society (JGS) for the Preparation of Soil Specimens for Triaxial Tests (JGS 0520-2009), the Method for Cyclic Undrained Triaxial Tests on Soils (JGS 0541-2009) and the Method for Cyclic Triaxial Tests to Determine Deformation Properties of Geomaterials (JGS 0542-2009). The procedure for the tests is as follows.

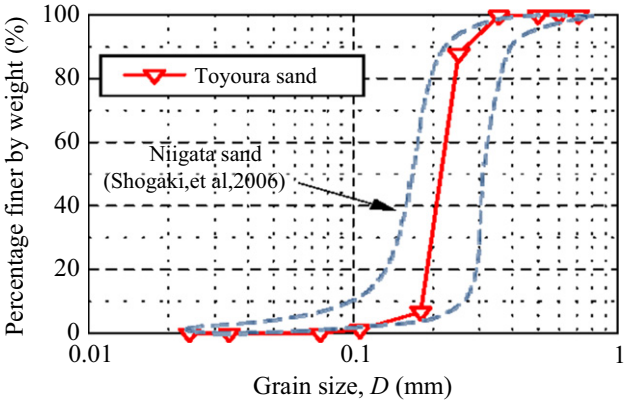

Fig. 1. Grain size distribution curves.

The specimen for the Toyoura sand is 50 mm in diameter (d) and 100 mm in height (h). The specimen for the Niigata sand, obtained from the 45-mm sampler, is 48 mm in d and 96 mm in h since the inner diameter of the sampler is 48 mm[1] . The liquefaction strength and the initial modulus of rigidity from cyclic triaxial tests ($G_{0(CTX)}$) decreased with the decreasing specimen diameter caused by the effect of membrane penetration. However, the effect of membrane penetration is negligible. This is because the exposed specimen can be trimmed to have a smooth surface (Shogaki et al., 2006). The testing conditions are summarized in Table 2.

The confined pressure (σ'_c) for a Toyoura sand specimen under consolidation is 100 kPa. The confined pressure is set to the *in situ* effective stress of the specimen for the Niigata sand. The frequency under cyclic loading is 0.1 Hz for measuring $G_{0(CTX)}$ and 0.5 Hz for the liquefaction tests. The cyclic loading for measuring $G_{0(CTX)}$ is controlled with an axial strain of less than 1×10^{-5} μm.

2.2. Penetration testing using semicircular tubes

These tests utilize the tubes of both the 45-mm and the 75-mm samplers; they are stainless steel tubes 60 cm in length, 1.5 mm in thickness and split lengthwise by a microlaser. Fig. 2 shows the step-by-step process for the measurement of the void ratio. The model testing procedure for the Toyoura sand is as follows

(1) Toyoura sand is hand-packed in a vinyl pipe to a predetermined relative density, and the targets are laid out on the surface in a grid pattern.
(2) The upper surface of the sand-filled pipe is set to be flush with the surface of the watertank using wedges.

[1]The 45-mm sampler has two inter-changeable tubes, one with a 45-mm inner diameter and the other with a 48-mm inner diameter.

Table 1
Results of grain size distribution tests.

Soil	Toyoura	Niigata (Shogaki et al., 2006)
Soil particle density ρ_s (g/cm^3)	2.653	2.693
Void ratio e	0.69～0.95	0.73～0.91
Gravel (%)	0	0～0.4
Sand (%)	100	93.2～99.1
Silt and clay (%)	0	0.6～6.8
Maximum grain size (mm)	0.85	0.85～4.75
Uniformity coefficient U_C	1.5	1.5～2.2
Curvature coefficient U'_C	0.94	1.0～1.2

Table 2
Testing conditions.

Relative density, D_r (%)	30	56	66	76	90	98
Back pressure (kN/m^2)	200	200	200	200	400	400
Initial modulus of rigidity from CTX, G_0	Frequency 0.25 Hz (Sin wave) $(\varepsilon_a)_{SA}=0.001 \sim 0.005\%$					
Liquefaction test from CTX	Frequency 0.50 Hz (Sin wave) $(\varepsilon_a)_{SA} < 10\%$					
B value	$B > 0.95$					

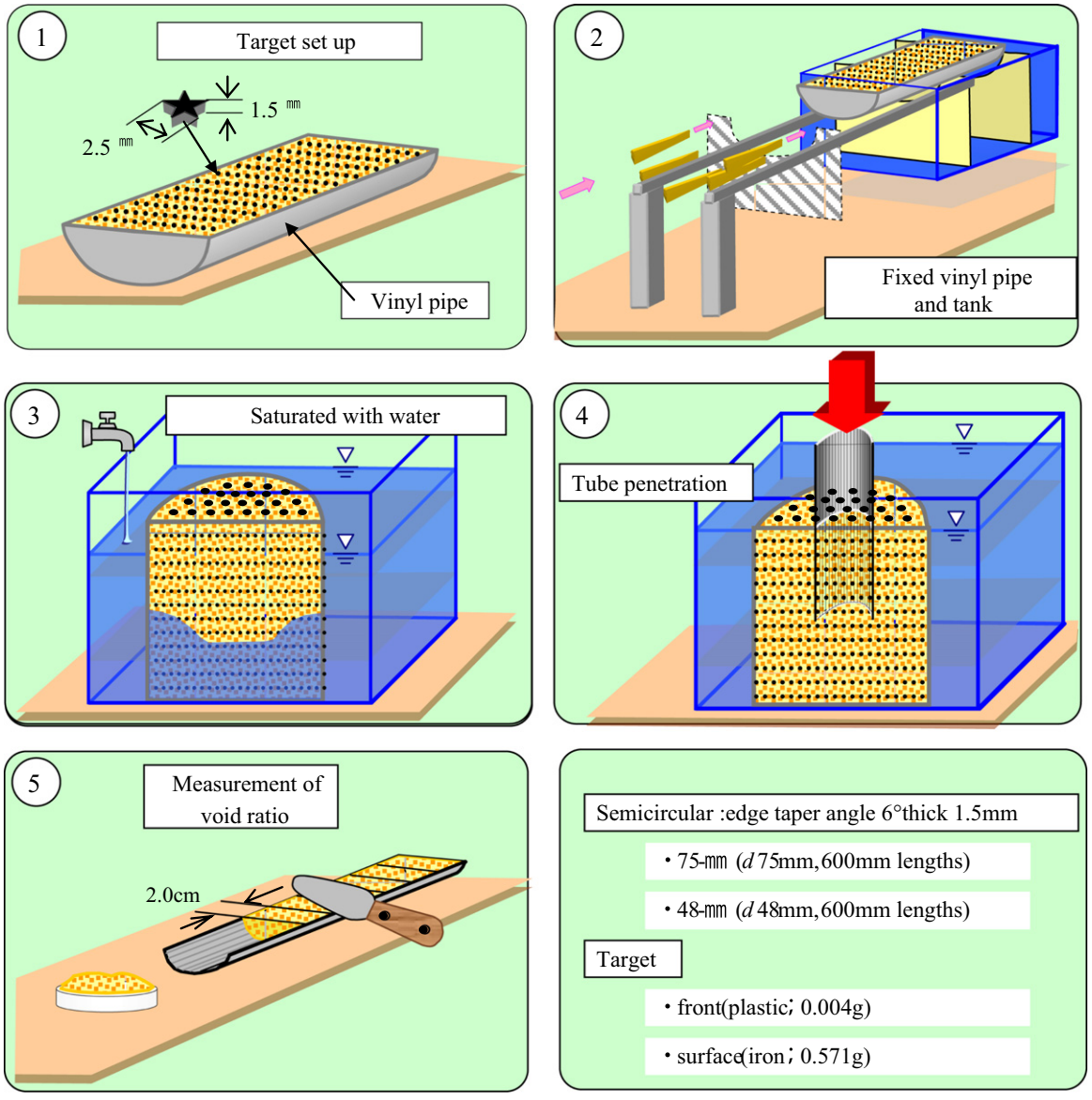

Fig. 2. Model testing procedure for Toyoura sand.

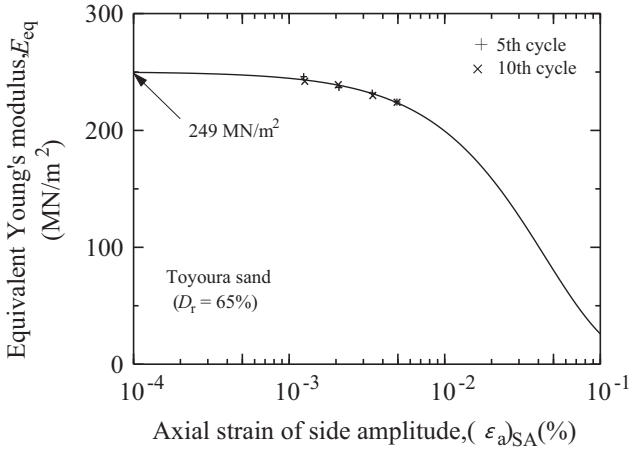

Fig. 3. Relationship between equipment's Young's modulus and $(\varepsilon_a)_{SA}$ (Toyoura sand).

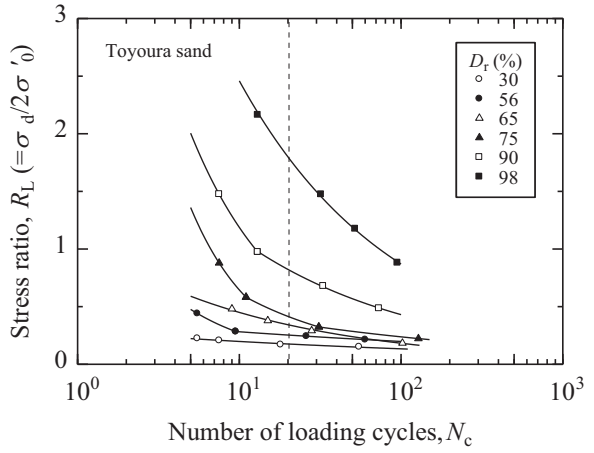

Fig. 4. Relationship between stress ratio and N_c (Toyoura sand).

(3) The tank is then set up so that the inserted sample is in a vertical position and is water-saturated.
(4) The semicircular sampling tube penetrates the sand to a depth of 32 cm and removes a sample.
(5) Finally, the void ratios are measured at 2-cm intervals of the sand sample.

For the model testing procedure, the benchmark relative densities of the Niigata sand (25%, 35%, 45%, 60%, 70% and 85%) are assumed for those of the Toyoura sand. The penetration speed (S_p) is set at about 5 cm/s for both of the sampling tubes since this is the actual situation when using a two-chambered hydraulic piston. The 75-mm sampler, S_p, is only about 2 cm/s (Shogaki et al., 2002).

3. Cyclic undrained triaxial tests

Fig. 3 shows the relationship between the equivalent Young's modulus (E_{eq}) and the axial strain $(\varepsilon_a)_{SA}$ of one side of amplitude determined from the fifth and tenth loading cycles (N_c) when the relative density (D_r) of the Toyoura sand is at 65%. $G_{0(CTX)}$ is determined as 83 (=249/3) MN/m^2 from E_{eq}=249 MN/m^2 at $(\varepsilon_a)_{SA}=10^{-4}$% using the Hardin and Drnevich model (JGS 0542-2009) for the plots of E_{eq} and $(\varepsilon_a)_{SA}$. Other $G_{0(CTX)}$ values of D_r=30%, 56%, 65%, 75%, 90% and 98% are obtained in the same manner. The relationship between the stress ratio ($R_L=\sigma'_d/2\sigma'_c$) and N_c in the liquefaction tests for the samples of D_r=30%, 56%, 65%, 75%, 90% and 98% of the Toyoura sand are shown in Fig. 4. The liquefaction strengths R_{L20} (R_L under N_c=20), determined from Fig. 4 and $G_{0(CTX)}$, are plotted against D_r for samples of Toyoura sand, as shown in Fig. 5. The regression curves for the plots of R_{L20} and $G_{0(CTX)}$ can be used as typical curves for the relationship among R_{L20}, $G_{0(CTX)}$ and D_r for Toyoura sand.

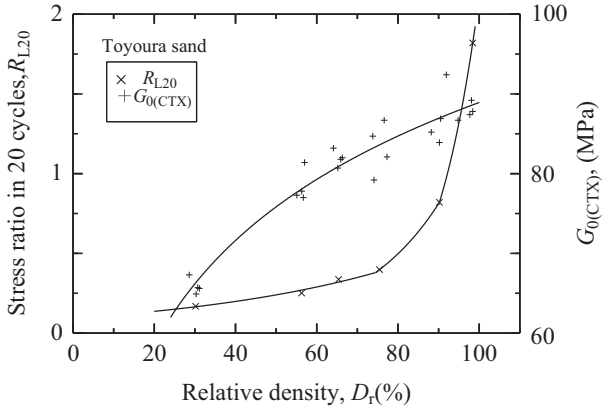

Fig. 5. Relationship among R_{L20}, G_{CTX} and D_r (Toyoura sand).

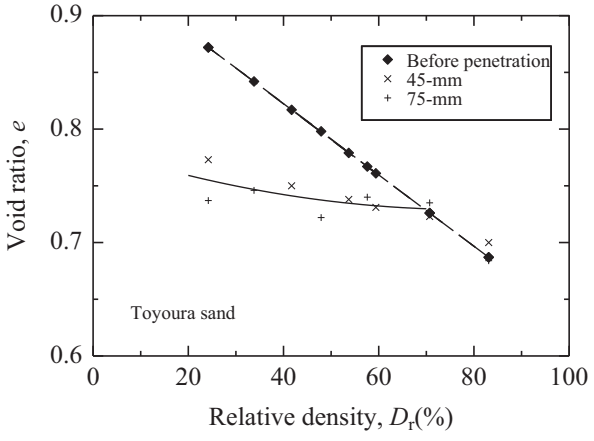

Fig. 6. Relationship between e and D_r (Toyoura sand).

4. Conventional method for estimating *in situ* dynamic strength and deformation properties of sand samples obtained from tube sampling

Fig. 6 shows the relationship between e and D_r for Toyoura sand in the model tests. The decreases (×,+) in e after the tube penetration from the initial void ratio (e_0)

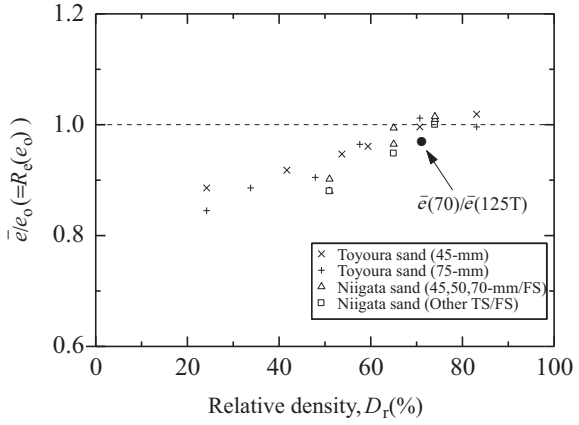

Fig. 7. Relationship between e/e_0 and D_r (Toyoura sand).

(♦) and before the tube penetration are greater for loose soils with smaller D_r, in which e_0 is defined as the void ratio after water saturation, as shown in Item 3 under the title of Penetration Testing Using Semicircular Tubes. The ratios $R_e(e_0)$ of the mean values ($\bar{e}$) of e for each 2-cm interval of sand sample, as shown in Fig. 2⑤, to the e_0 sampled from the semicircular tube penetration, are plotted against D_r in Fig. 7. The $R_e(e_0)$ obtained from the semicircular tube is about 1.0 when $D_r > 70\%$ and the mean values for $R_e(e_0)$ of $D_r = 59\%$, 53%, 42%, 34% and 24% are 0.94, 0.94, 0.92, 0.88 and 0.85, respectively. These changes are unrelated to the tube diameter. To compare the model tests with the results for Niigata sand deposits, the ratios $R_e(e_0)$ (△) of the e_0 obtained from the 45-mm, 50-mm and 70-mm samplers to those of FS at Meike Elementary School in Niigata City, together with the results of other tube sampler values (TS) (□), are also shown in Fig. 7. The $R_e(e_0)$ values of $D_r = 51\%$ for the 45-mm, 50-mm and 70-mm samplers for Niigata sand change to 0.90 and 0.88 for other TS. Therefore, there is a decrease in the void ratio due to the tube penetration. The mean values $R_e(e_0)$ of $D_r = 65\%$ and 74% are 0.97 and 1.01, respectively. The $(e_{(70)}/e_{(125T)})$ value of D_r72%, shown at (●), is the ratio of e for 70-mm to 125-mm triple tube samplers. The $R_e(e_0)$ value of this plot is 0.96; it is caused by increasing the void ratio due to the tube's cutting edge. Niigata sand (△) (Shogaki et al., 2002) at $D_r > 51\%$ consists of natural deposits sampled from a circular cylinder tube, and the relationship between R_e and D_r has the same tendency as a semicircular tube. It can be seen from Fig. 7 that the void changes in a sample from a semicircular tube are similar to those of a sampling of Niigata natural deposits and the model tests on Toyoura sand. Therefore, semicircular tube penetration for Toyoura sand can simulate circular cylinder tube penetration for Niigata sand deposits.

The ratios (R_e and RD_r) of e_0 and $D_{r(o)}$ before penetration to e and D_r, obtained from a semicircular tube for Toyoura sand in Fig. 7, are plotted against D_r in Fig. 8. R_e and RD_r values are 1.0 at $D_r \fallingdotseq 70\%$ and the measured values for e and D_r, where $D_r < 70\%$ are under/overestimated, respectively,

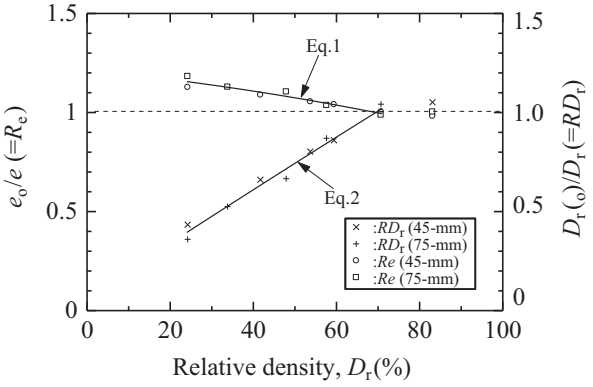

Fig. 8. Relationship among Re, RD_r and D_r (Toyoura sand).

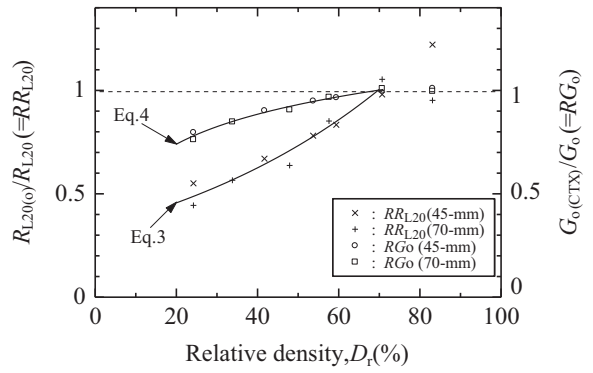

Fig. 9. Relationship among RR_{L20}, RG_0 and D_r.

due to the increase in density by sampling. Both regression curves for the plots in Fig. 8 can be used as the revision curves for the *in situ* e and D_r from the values measured with the circular cylinder tube.

The ratios (RR_{L20} and $RG_{0(CTX)}$) of R_{L20}(o) and $G_{0(CTX)}$ before penetration to the R_{L20} (×) and $G_{0(CTX)}$ (+) values, equivalent to D_r obtained from a semicircular tube, are read from the curves in Fig. 5 and plotted against the D_r in Fig. 9. The R_{L20} and $G_{0(CTX)}$ values increase with an increasing D_r when $D_r < 70\%$, since the e value decreases with tube penetration. The correlation equations and correlation coefficients (r) for R_e, RD_r, RR_{L20} and $RG_{0(CTX)}$ are shown in Table 3. *In situ* e ($=e_0$), D_r ($=D_r$(o)), R_{L20} ($=R_{L20}$(o)) and $G_{0(CTX)}$ values can be estimated from the measured e, D_r, R_{L20} and $G_{0(CTX)}$ values multiplied by the correlations in Table 3.

This is an economically feasible method, utilizing changes in density for estimating the *in situ* dynamic strength and deformation properties of sand samples obtained from a circular cylinder tube.

5. Applicability of proposed method for Niigata sand deposits

A series of *in situ* samplings and investigations for Niigata sand deposits were conducted at Meike Elementary School in Niigata City by Yoshimi et al. (1989), the Japanese Society for Soil Mechanics and Geotechnical

Table 3
Correlation equation for estimating *in situ* e, D_r, R_{L20} and G_0 values.

Fig.	Regression equation		Correlation coefficient
8	$Re = 1.214 - 0.00205D_r - 0.0000147D_r^2$	(1)	0.963
8	$RD_r = 0.076 + 0.013D_r - 0.0000051D_r^2$	(2)	0.991
9	$RR_{L20} = e^{(0.01579Dr - 1.101)}$	(3)	0.948
9	$RG_0 = 0.209 \ln D_r + 0.114$	(4)	0.991

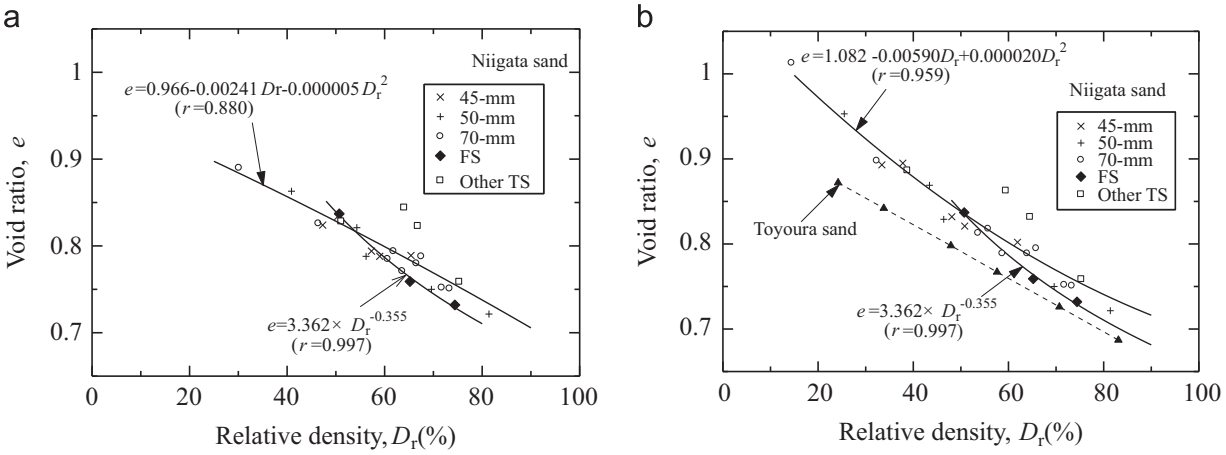

Fig. 10. Relationship between e and D_r (Niigata sand). (a) Using measured values. (b) Using Eq. (2).

Table 4
Specifications of samplers used in the 2000 investigation.

Sampler	45-mm	50-mm	70-mm
Length of sampler (mm)	1340	1680	1165
Weight of sampler (kg)	10.6	12.8	21.4
Greatest outside diameter of sampler (mm)	60	60	90
Length of tube (mm)	600	800	950
Greatest outside diameter of tube, D_2 (mm)	52	56	76
Inside diameter of tube, D_1 (mm)	48	50	70
Thickness of tube (mm)	2	3	3
Edge taper angle (deg.)	5.4	6.6	31.0
Thickness of edge (mm)	0.2	0.2	0.2
Inside clearance (mm)	0	0	0
Area ratio, C_a (%)	17	25	18
Maximum sample length (mm)	535	735	796

Engineering (1988) and Shogaki et al. (2002). The applicability of the proposed method for Niigata sand deposits is discussed along with the results of tests on samples obtained from each TS. The relationship between e and D_r for Niigata sand is shown in Fig. 10. Fig. 10(a) shows the relationship between e and D_r, using the measured values. The sampler specifications are shown in Table 4. The plots for e and D_r of TS for Niigata sand are estimated as *in situ* e and D_r using Eqs. (1) and (2), as shown in Table 3, together with the FS of Niigata sand deposits and Toyoura sand, and are also shown in Fig. 10(b). The plots for $D_r < 70\%$ of TS for Niigata sand moved to sites having larger e and smaller D_r, as shown in Fig. 10(b), and the regression curve for all the TS plots is almost parallel to the curve for Toyoura sand and is the reason why the e values of Toyoura sand are about 0.05 smaller than those of Niigata sand under the same D_r. The e values of the other TS (□) are larger than those of the 45-mm, 50-mm and 70-mm samplers.

Fig. 11 shows the relationship between the N value obtained from SPT and D_r for Niigata sand. The D_r values shown in Fig. 11(b) are revised by Eq. (2) in Table 3. The N values are converted to N_1 values using Eq. (5), which was adopted by the Japan Public Highway Corporation (Specifications for Highway Bridges, 2003) in order to consider the effective overburden pressure.

$$N_1 = 170N/(\sigma'_v + 70) \quad (5)$$

The results of FS and TS from the 1986 and 1987 investigations, as well as the results of Eq. (6) by Meyerhof (1957), are converted to N_1 and are also shown in Fig. 11.

$$D_r = 208\sqrt{\frac{N}{\sigma'_{vo} + 69}} \quad (6)$$

The straight line, mentioned as Eq. (7) in Fig. 11, is a regression line obtained from the least squares method for the plots of the FS sample. The D_r values of FS increase

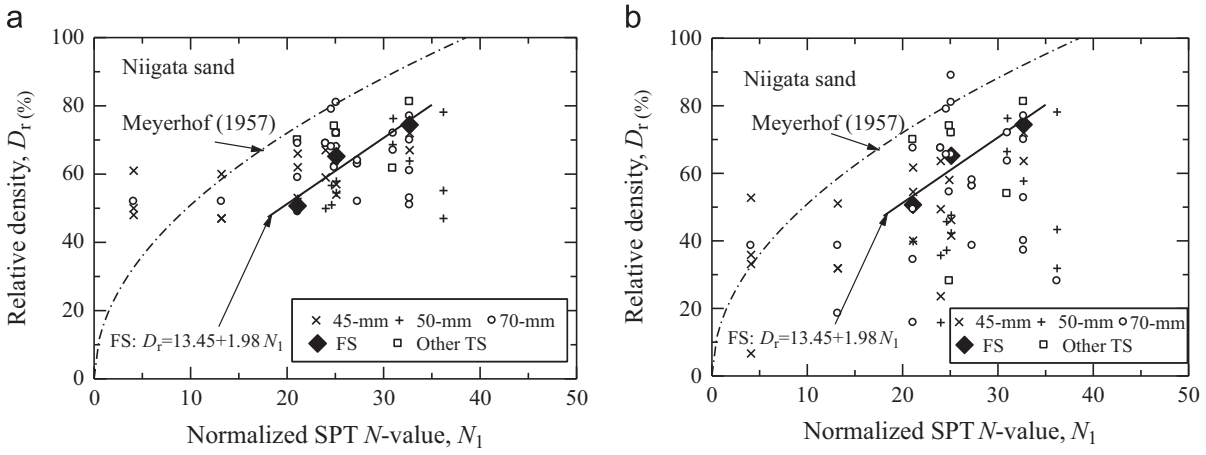

Fig. 11. Relationship between D_r and N_1. (a) Using measured values. (b) Using Eq. (2).

with an increasing N_1,

$$D_r = 13.45 + 1.98N_1 \quad (7)$$

where the plots (◆) for FS show the mean values of D_r and the other plots show the mean value ($\overline{D}_r$) of D_r for each specimen. All plots, except for that of $N_1 < 5$, are located at the lower part of Meyerhof's curve. This curve does not consider the effect of fine grained soil and was proposed about 50 years ago. Therefore, the curve cannot describe the actual circumstances since sampling techniques have improved since then.

The void ratio (e_c) is determined using Eq. (1). After the consolidation of each specimen, the *in situ* values $\overline{D}_{r(a)}$ of D_r, estimated by Eq. (2), and the $\overline{D}_{r(b)}$ values, obtained from the TS samples, are plotted against z in Fig. 12. The broken lines in Fig. 12 are the estimated lines for $\overline{D}_{r(b)}$ and $\overline{D}_{r(a)}$ obtained from Eq. (7). The $\overline{D}_{r(b)}$ and $\overline{D}_{r(a)}$ values obtained from Eq. (6) are shown as solid lines in Fig. 12. This is reflected in Fig. 11, as all plots are located on the lower part of the solid line of Eq. (6), as proposed by Meyerhof (1957). The $\overline{D}_{r(a)}$ values of $z=(6\sim10)$ m for the TS samples are similar to those of the FS samples and very close to the estimated line of Eq. (7). The change in density, caused by sampling, is modified to an *in situ* condition by this proposed method using Eq. (2). The $\overline{D}_{r(a)}$ values are overestimated. However, for a specimen obtained from the same tube, the plots are determined to come from further up in the sampling tube and are located close to the estimated line by Eq. (7) for the 50-mm sample at $z \fallingdotseq 5.5$ m. The $\overline{D}_{r(a)}$ value for the samples obtained from the 45-mm sampler at $z \fallingdotseq 2$ m move closer to the broken line, as shown in Eq. (7). This means that the decreasing D_r values, caused by the loss of the sample near the cutting edge, are confined to narrow limits. The plots for the $\overline{D}_{r(b)}$ of the TS sample of $z > 6$ m have larger values than the estimated ones by Eq. (7) and are caused by the increasing sample density due to tube penetration at these depths. The $\overline{D}_{r(a)}$ values of the plots, from the 50-mm and 70-mm samples at $z \fallingdotseq 12$ m, are smaller than those of Eq. (7). It is known that the sample densities obtained from TS, for soil having large N values, decrease because of tube penetration and withdrawal. This was the situation for the sample at $z \fallingdotseq 12$ m. The change in density, caused by the sampling, can be modified appropriately to an *in situ* condition by this proposed method using Eq. (2).

6. Applicability of liquefaction strength by laboratory tests and site investigations

Before and after revisions of the R_{L20} values, using Eq. (3) for Toyoura sand, the stress ratios are plotted against D_r together with Toyoura sand in Fig. 13(a) and (b). The D_r values in Fig. 13 are revised to *in situ* values from the measured values using Eq. (2). Overall, the R_{L20} values of FS are similar to those of Toyoura sand. However, the R_{L20} values obtained from TS are 0.05∼0.1 smaller than those of FS and Toyoura sand. The R_{L20} values obtained from other samplers (□) are 0.1 smaller than those of FS and Toyoura sand, particularly in the plots showing $D_r=37\sim82\%$. The difference in R_{L20} for each sampling method reflect the difference in e, as shown in Fig. 10. The relationship between the R_{L20} and D_r values obtained from FS, static penetration-tube samplers (45-mm, 50-mm and 70-mm), rotary triple-tube samplers (other TS) and Toyoura sand are parallel to each other, as shown in Fig. 13(b) after revision. The R_{L20} values increase with increasing D_r values since e decreases with increasing D_r values. The relationship between the estimated R_{L20} and D_r values are parallel, whereas the measured values are not. Therefore, this method, which utilizes our proposed Eqs. (2) and (3), is a more accurate simulation of the *in situ* conditions.

The sample quality obtained from FS and TS is discussed from a comparison of R_{L20} estimated from site investigations and those measured and estimated values by Eq. (3) for the results of CTX.

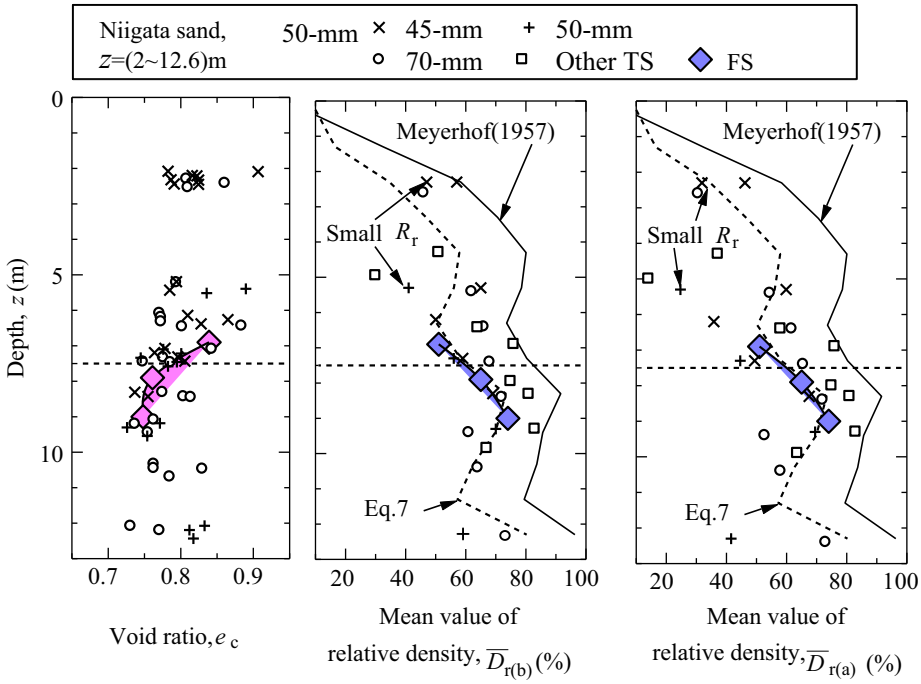

Fig. 12. Relationship among e_c, $\overline{D}_{r(b)}$ and $\overline{D}_{r(a)}$ and depth (Niigata sand).

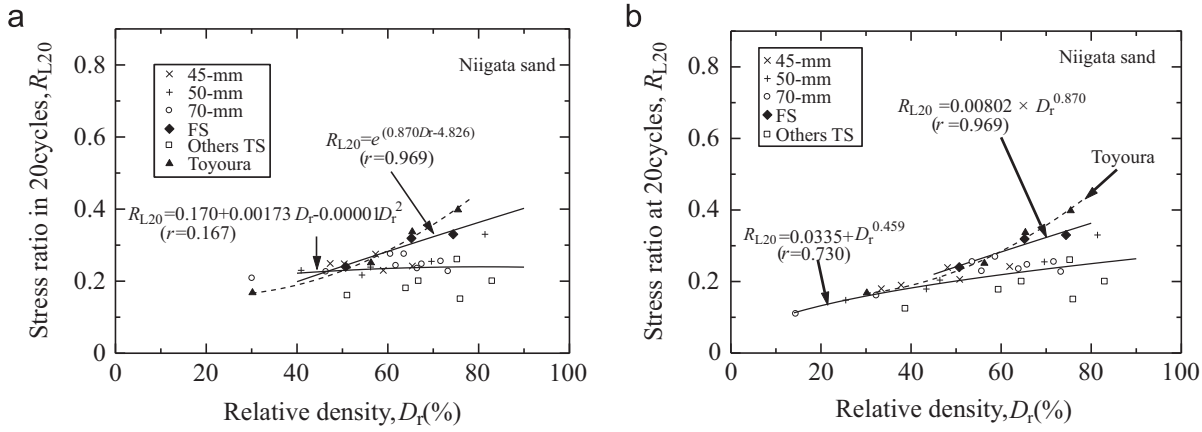

Fig. 13. Relationship between R_{L20} and D_r (Niigata sand). (a) Using measured values. (b) Using Eqs. (2) and (3).

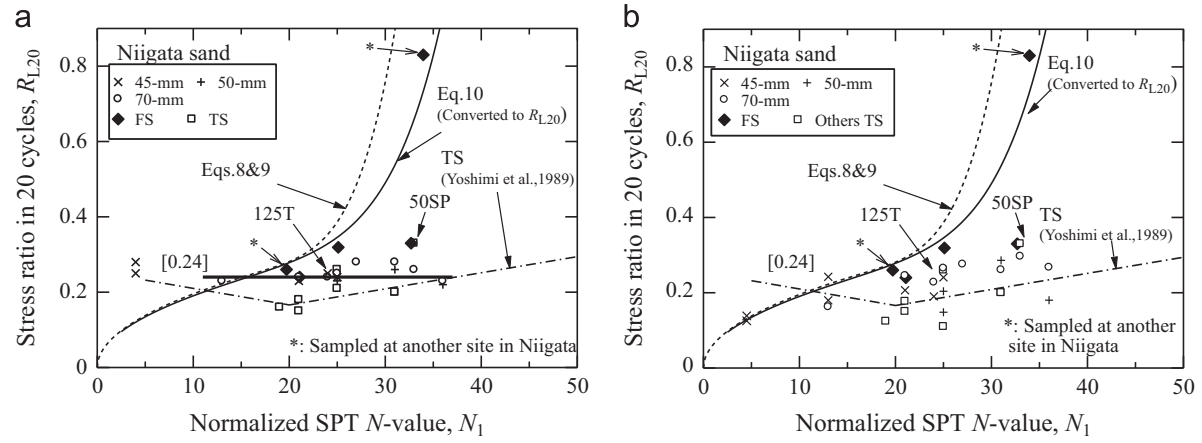

Fig. 14. Relationship between R_{L20} and N_1 (Niigata sand). (a) Using measured values. (b) Using Eq. (3).

6.1. Comparison of R_{L20} values estimated from N values of SPT and measured ones from CTX

Concerning the relationship between N and R_{L20} for the conventional estimation method of the liquefaction strength in the Specifications for Highway Bridges (2003), Eqs. (8) and (9) are used for sandy soil, which has a small F_c value.

$$R_{L20} = 0.0882\sqrt{N_1/1.7} \quad (N_1 < 14) \tag{8}$$

$$R_{L20} = 0.0882\sqrt{N_1/1.7} + 1.6 \times 10^{-6} \times (N_1 - 14)^{4.5} \quad (N_1 \geqq 14) \tag{9}$$

Tokimatsu and Yoshimi (1983) used Eq. (10) to determine the relationship between N and R_{L15} (R_L under $N_c = 15$) for $F_c \leqq 5\%$ for the FS sample.

$$R_{L15} = 0.45 \times \left\{ \frac{16\sqrt{N_1}}{100} + \left(\frac{16\sqrt{N_1}}{97 - 19\log DA} \right)^{14} \right\} \tag{10}$$

where N_1 is the converted N value, as shown in Eq. (5).

Fig. 14(a) shows the relationship between R_{L20} and N_1, obtained from Eqs. (4) and (5), and the measured values. The regression lines obtained from the test results, in which Yoshimi et al. (1989) and Yoshimi (1994) carried out sampling at the same site as our research and at another site in Niigata City for the TS samples, are also shown in Fig. 14 with a dotted line. Yoshimi et al. (1989), Tokimatsu and Yoshimi (1983) and Yoshimi (1994) used liquefaction strength R_{L15} in their papers. Therefore, R_{L15} is converted to R_{L20}, using Eq. (11) by Tatsuoka et al. (1980).

$$R_L = R_{L20}(N_c/20)^{-0.1-0.1\log_{10} DA} \tag{11}$$

where $R_{L20} \fallingdotseq 0.95R_{L15}$. The R_{L20} values, obtained from the design code for road bridges and Yoshimi et al. (1989) and Yoshimi (1994), preliminarily increase in the area of $N_1 = 15 \sim 22$ and exponentially increase in the area of $N_1 > 22$ in Fig. 14(a). However, the measured values differ widely from this tendency. The characteristics of the measured values, shown in Fig. 14(a), are summarized as follows:

(1) The R_{L20} values are almost constant for the N_1 values, and the mean value is 0.24.
(2) The measured R_{L20} values under $N_1 \fallingdotseq 13$ are larger than those estimated from Eq. (10) by Tokimatsu and Yoshimi (1983) and from Eqs. (8) and (9) from the Specifications for Highway Bridges (2003).

Our conclusions are as follows:

(1) The R_{L20} values obtained from the 45-mm, 50-mm and 70-mm samplers are overestimated in the areas of less than $N_1 \fallingdotseq 20$ and are caused by the increased density when the sampling tube penetrates the soil. They are underestimated in the areas of greater N_1 values and caused by the decreased density and changes in the grain arrangement due to sample disturbance.
(2) The D_r values obtained from the 45-mm, 50-mm and 70-mm samplers are similar to those of the FS in the area of $N_1 = 20 \sim 35$. However, the small change in the grain arrangement, caused by the shear history of the tube penetration and extraction, has influenced the shape of the liquefaction curve.
(3) The R_r values from the 45-mm and 50-mm samplers were larger than those from the 70-mm sampler due to the difference in tube penetration force and speed (Shogaki et al., 2002). The R_{L20} values obtained from the 45-mm, 50-mm and 70-mm samplers are almost similar. However, the R_{L20} values obtained from the other TS are 0.2 smaller than those obtained from the 45-mm, 50-mm and 70-mm samplers. The sampling method and the differences between rotary and static penetration samplers determine the sample quality. The characteristics of the estimated *in situ* R_{L20} values by Eq. (3), shown in Fig. 14(b), are summarized as follows:
(1) The R_{L20} values from other samplers (□) are smaller than those estimated by Yoshimi et al. (1989).
(2) The mean value of R_{L20} obtained from TS (× , + , ○) is parallel to the regression line for FS.
(3) The R_{L20} values increased with the increasing N_1 values since the soil strength increased along with the increasing N_1 values.

Therefore, the change in R_{L20}, caused by sampling, can be modified to a more accurate simulation of the *in situ* conditions by using Eq. (3).

6.2. Comparison of R_{L20} values estimated from q_c of CPT and those measured from CTX

The CPT can continuously measure the changes in soil at various depths. The q_c values at each 5-cm depth interval were measured in the 2000 investigation in accordance with the Japanese Geotechnical Standards for electric cone penetration tests (JGS 1435-2003). Therefore, since accurate liquefaction strength can be estimated by utilizing the q_c values, this makes their use concerning reliable and cost-effective construction engineering most important (Shogaki and Kumagai, 2008). The estimation methods by Ishihara (1985) and Suzuki et al. (1995) are used for a comparison of the R_{L20} in this study. The method by Suzuki et al. (1995) includes the test results for the samples obtained from the sampling site of these authors. The q_c values obtained from their method eliminate the effective overburden pressure (σ'_{vo}) using Eqs. (12) and (13).

$$q_{t1} = [1.7/\{(\sigma'_{vo}/p_a) + 0.7\}] \times q_t \tag{12}$$

$$q_{t1} = q_t/\sqrt{\sigma'_{vo}} \tag{13}$$

where q_t is the modified tip resistance of the cone on the q_c value for water pressure and q_{t1} is the value eliminated by σ'_{vo} from q_t. The p_a is 98.1 kPa. The q_{t1} values obtained from Eqs. (12) and (13) are almost similar and in the range of $\sigma'_{vo} > 30$ kPa. Therefore, Eqs. (12) and (13) are treated alike in this study.

The relationship between q_{t1} and R_{L20} is shown in Fig. 15. Figs. 15(a) and (b) show before and after revisions for R_{L20}, using Eq. (3). In Fig. 15(a), the regression curve by Ishihara (1985) is far removed from the plots of the FS samples and from the regression curve by Suzuki et al. (1995). Ishihara (1985) used the samples, $N<20$ with $F_c \leqq 10\%$, obtained from the Osterberg piston sampler, the original hydraulic piston sampler, for the regression curve. The R_{L20} values obtained from Ishihara's regression curve are overestimated, since the density increased with tube penetration, as described in a former section of this paper. The R_{L20} values obtained from the FS sample and by Suzuki et al. (1995) increased in this paper with an increasing q_{t1}, but the measured values from the 45-mm, 50-mm and 70-mm samplers do not have those tendencies. However, the R_{L20} values obtained from the 45-mm and 50-mm samplers are similar to those of the FS sample. As per a prior discussion on the N_1 value, the estimated R_{L20} values from q_{t1} for the 45-mm and 50-mm samplers are almost similar to that for the 70-mm sampler.

The characteristics of the estimated *in situ* R_{L20} values by Eq. (3), shown in Fig. 15(b), are summarized as follows:

(1) The regression curves of R_{L20} for FS, static penetration-tube samplers (45-mm, 50-mm and 70-mm) and rotary triple-tube samplers (other TS) increased with an increasing q_{t1}.
(2) The regression curves for R_{L20}, obtained from TS ($\times$, +, ○) and other TS (□), are $R_{L20} \fallingdotseq 0.05$ and $R_{L20} \fallingdotseq 1.0$, smaller than those of FS.

6.3. Comparison of R_{L20} values estimated from velocity of secondary wave of P/S logging and those measured from CTX

Robertson et al. (1992) and Tokimatsu and Uchida (1990) are well known for their estimation methods of the liquefaction strength using the secondary wave velocity

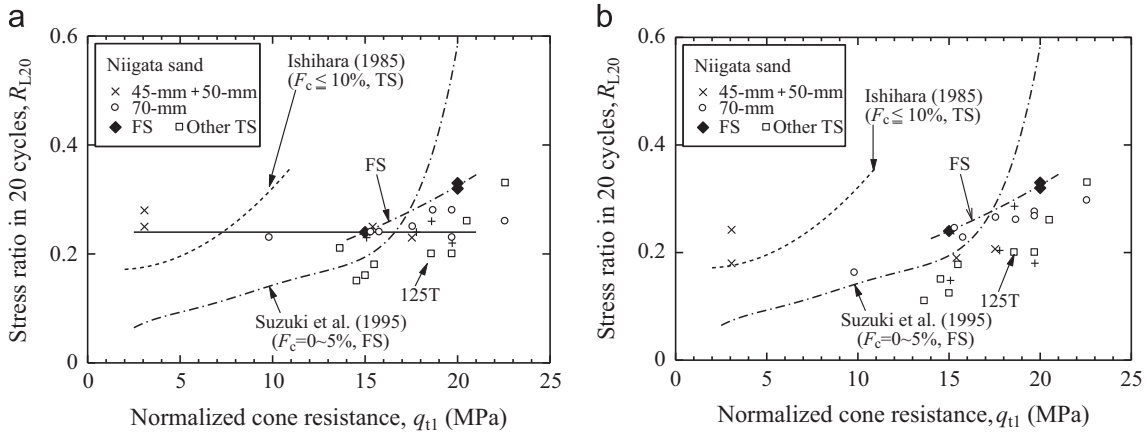

Fig. 15. Relationship between R_{L20} and q_{t1} (Niigata sand). (a) Using measured values. Using Eq. (3).

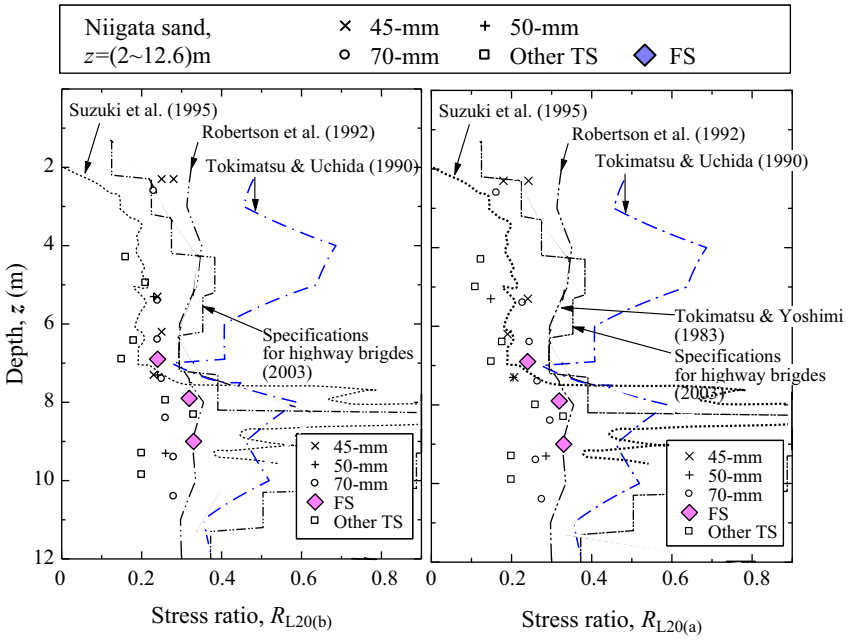

Fig. 16. Relationship between R_{L20} and depth (Niigata sand).

(V_s) from the P/S logging. The measurement interval of V_s, from the P/S logging, is the same as that of SPT. However, the surface wave exploration method can measure the V_s not only in a vertical direction, but also in a horizontal one near the ground surface.

The Robertson et al. (1992) method is derived from the shear stress ratio of the earthquake motion calculated from the normalized velocity of the secondary wave (V_{s1}), for which the effect of σ'_{vo} is eliminated by Eq. (14).

$$V_{s1} = V_s/(\sigma'_{vo}/p_a)^{0.25} \tag{14}$$

The R_{L20} values are estimated by the figure mentioned in Robertson et al. (1992), using the V_{s1} obtained from Eq. (14) in this study.

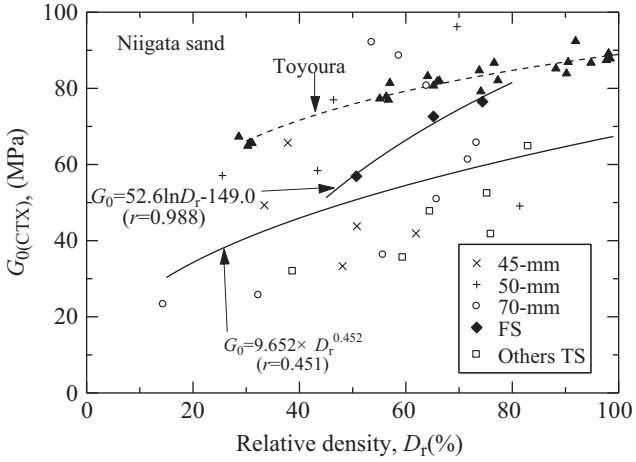

Fig. 17. Relationship between $G_{0(CTX)}$ and D_r.

The *in situ* R_{L20} values, estimated from the methods by Suzuki et al. (1995) and Robertson et al. (1992), and the R_{L20} values, obtained from Fig. 14, are plotted against depths in Fig. 16. The $R_{L20(a)}$ values on the right-hand side of Fig. 16 are revised by Eq. (3); the left-hand side shows the $R_{L20(b)}$ values before revision. The $R_{L20(b)}$ values obtained from the TS sampling, including the 45-mm and 50-mm samplers, underestimate the *in situ* values. The R_{L20} values estimated from Suzuki et al. (1995) closely match the measured values. The R_{L20} values obtained from the FS sample closely match those of the *in situ* values. The mean values of $R_{L20(a)}$, obtained from TS (×, +, ○) and other TS (□), are $R_{L20(a)} \fallingdotseq 0 \sim 0.05$ and $R_{L20(a)} \fallingdotseq 0.1 \sim 0.2$ smaller than those of FS at the depth of 7∼9 m. In the Specifications for Highway Bridges (2003), the R_{L20} values do not show accurate *in situ* values.

6.4. Effect of sampling method on initial modulus of rigidity in Niigata sand

The sample quality obtained from the 45-mm, 50-mm, 70-mm, FS and other TS samplers is evaluated from G_{BE} and $G_{0(CTX)}$ before the liquefaction test for each specimen. The D_r and G_0 values, after revision by Eqs. (2) and (4), are plotted in Fig. 17. The r value for the regression curve of the plots obtained from the 45-mm, 50-mm, 70-mm and other TS of Niigata sand is as small as 0.451, and the G_0 values increase with an increasing D_r, as they also do so for Toyoura sand (▲). However, the G_0 values of Niigata sand are smaller by about 25 MPa. The plots of FS are located between both curves. Before $G_{CTX(b)}$ and after $G_{CTX(a)}$ values, revised by

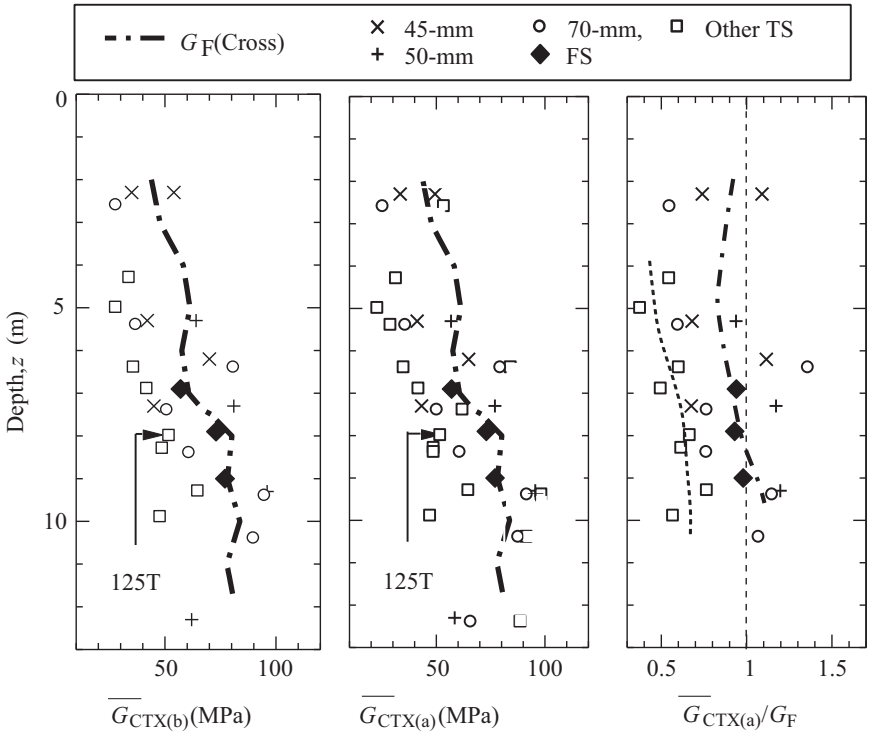

Fig. 18. Relationship among $\overline{G}_{CTX}$ and $\overline{G}_{BE}/\overline{G}_F$ and depth.

Eq. (4), together with $G_{CTX(a)}/G_F$ obtained from the TS and FS samples, are plotted against the depths in Fig. 18. The plots of $G_{CTX(b)}$ for the FS sample are located close to the curve for the depth of G_F, and the $\overline{G}_{CTX(a)}/G_F$ of the FS sample is almost 1.0. However, the $\overline{G}_{CTX(a)}/G_F$ values obtained from the 45-mm, 50-mm and 70-mm samplers, as shown by the solid line, are in the range of 0.8 to 1.1 and the mean value is 0.955 and greater than those of other TS samplers (□), as shown by the dotted line. However, the $\overline{G}_{CTX(a)}/G_F$ ratios of the other TS samplers are in the range of 0.45∼0.65 and are (30∼45)% of the G_F, regardless of the small $\overline{D}_r$ values. They coincide with the results for R_{L20} in Figs. 13, 14 and 15. The $G_{CTX(b)}$ values are revised to a maximum of 20% by Eq. (4) in response to D_r, and the $G_{CTX(a)}$ values obtained from the 45-mm, 50-mm and 70-mm samplers are similar to those of G_F. The $G_{CTX(a)}$ values for the 45-mm and 50-mm samplers, having similar R_{L20} values to the FS samples, are also similar to G_F. Therefore, the change in G_0, caused by sampling, can be appropriately modified to an *in situ* condition using Eq. (4).

The N, e_0, D_r, and R_{L20} values of the Niigata Airport sand differ from those of the Meike Elementary School sand. However, the dynamic strength property of the Niigata Airport sand remains consistent with that of the Meike Elementary School sand concerning the *in situ* conditions using the proposed method (Shogaki et al., 2010). The FS sample can be kept in an *in situ* condition since the sample disturbance is smaller for clean sand. Therefore, the small $R_{L20(a)}$ and $G_{0(CTX)}$ values from the TS samples, shown in Figs. 13(b)–16(b) and Fig. 17, are caused by an increasing D_r, the arrangement of the sand particles, the aging effect, *etc.*

7. Conclusions

The conclusions obtained in this study are summarized as follows:

(1) An economically feasible method is proposed for estimating the *in situ* void ratio (e_0), the relative density (D_r) and the stress ratio (R_{L20}) in a 20-cyclic time frame and the initial modulus of rigidity (G_0) of sand samples utilizing density changes.

(2) The R_{L20} values increased with increasing D_r values since the e decreased with increasing D_r values. The relationship between the R_{L20} and D_r values, obtained from estimated *in situ* R_{L20} and D_r values, were parallel, whereas the measured values were not. Therefore, this method, utilizing our proposed Eqs. (2) and (3), is a more accurate simulation of the *in situ* conditions.

(3) The *in situ* R_{L20} estimated from the proposed method for sand samples from the 45-mm, 50-mm and 70-mm samplers and other tube samplers were 0∼0.05 and 0.1∼0.2, smaller than those of the frozen sample (FS) at the depth of 7∼9 m. The R_{L20} values from the Specifications for Highway Bridges (2003) were larger than those of the plots obtained from FS for Niigata sand deposits.

(4) The *in situ* G_0 estimated from the proposed method for sand samples obtained from the 45-mm, 50-mm and 70-mm samplers were in the range of 0.8∼1.1 of the *in situ* modulus (G_F) of initial rigidity and were calculated from the secondary wave velocity, the mean value being 0.955. However, the *in situ* G_0 values of other TS samplers were in the range of 0.45∼0.65 and were (30∼45)% of the FS. The *in situ* G_0 values for the 45-mm, 50-mm and 70-mm samplers, having R_{L20} values similar to the FS samples, were also similar to G_F for the Niigata sand deposits.

Therefore, changes in the dynamic strength and deformation properties, caused by sampling, can be modified appropriately to an *in situ* condition through this proposed method.

Notations

CTX	cyclic triaxial test
E_{eq}	equivalent Young's modulus
F_c	percentage of grain size smaller than 0.075 mm
FS	frozen sample
D_r	relative density
$D_{r(o)}$	relative density before tube penetration (*in situ*)
e	void ratio
$\overline{e}$	mean value of void ratio
e_c	void ratio after consolidation
e_0	initial void ratio before tube penetration (*in situ*)
G_0	initial modulus of rigidity
$G_{CTX(a)}$	G_0 estimated by Eq. (4) (after revisions)
$G_{CTX(b)}$	G_0 obtained from TS (before revisions)
$G_{0(CTX)}$	initial modulus of rigidity from cyclic triaxial test
R_{L15}	liquefaction strength under $N_c=15$
R_{L20}	liquefaction strength under $N_c=20$
$R_{L20(o)}$	liquefaction strength under $N_c=20$ before tube penetration (*in situ*)
$R_{L20(a)}$	R_{L20} estimated by Eq. (3) (after revisions)
$R_{L20(b)}$	R_{L20} obtained from TS (before revisions)
Re	e_0/e
$Re(e_0)$	$\overline{e}/e_0$
RD_r	$D_{r(o)}/D_r$
RG_0	$G_{0(CTX)}/G_0$
RR_{L20}	$R_{L20(o)}/R_{L20}$
R_r	sample recovery ratio
N	number of blows of the Standard Penetration Test (SPT)
N_1	N value considered the effective overburden pressure
N_c	number of loading cycles
q_c	tip resistance of the Cone Penetration Test (CPT)
q_t	modified tip resistance of the cone on the q_c value for water pressure
q_{t1}	eliminated value for the σ'_{vo} from q_t
S_p	penetration speed
TS	tube sampling

V_s secondary wave velocity
V_{s1} normalized V_s for the σ'_{vo}
σ_d cyclic deviation stress
$(\varepsilon_a)_{SA}$ axial strain of one side of amplitude
σ'_c effective confined pressure
σ'_{vo} effective overburden pressure
Δu excess water pressure

References

Ishihara, K., 1985. Stability of natural deposits during earthquakes. In: Proceedings of 11th ICSMGE, vol. 1, pp. 321–390.

Japan Geotechnical Consultant Association, 1998. Collaborative study on liquefaction of soils technical forum 1998, 341 p (in Japanese).

Japanese Geotechnical Society, 1988. A report on the sampling and evaluating sample quality methods for sand deposits, the soil sampling-committee of the Japanese Society for Soil Mechanics and Geotechnical Engineering, 71 p (in Japanese).

Japanese Geotechnical Society, 2009a. Method for cyclic triaxial test to determine deformation properties of geomaterials (JGS 0542-2009), Japanese standards for laboratory soil test methods—Standards and explanations, pp. 751–759 (in Japanese).

Japanese Geotechnical Society, 2009b. Preparation of soil specimens for triaxial tests (JGS 0520-2009), Japanese standards for laboratory soil test methods—Standards and explanations, pp. 553–557 (in Japanese).

Japanese Geotechnical Society, 2009c. Methods for cyclic undrained triaxial test on soils (JGS 0541-2009), Japanese standards for laboratory soil test methods—Standards and explanations, pp. 730–736 (in Japanese).

Japanese Geotechnical Society, 2004c. Method for electric cone penetration test (JGS 1435-2003), Japanese standards for geotechnical and geoenvironmental investigation methods—Standards and explanations, pp. 301–309 (in Japanese).

Meyerhof, G.G., 1957. Discussion for Session 1. In: Proceedings of the 4th ICSMFE, vol. 3, London, pp. 110.

Robertson, P.K., Woeller, D.J., Finn, W.D.L, 1992. Seismic cone penetration test for evaluating liquefaction potential under cyclic loading. Canadian Geotechnical Journal 29, 285–295.

Shogaki, T., 1996. A method for correcting consolidation parameters for sample disturbance using volumetric strain. Soils and Foundations 36 (3), 123–131.

Shogaki, T, 1997. A small diameter sampler with a two-chambered hydraulic piston and the quality of its samples. In: Proceedings of the Fourteenth International Conference on Soil Mechanics and Foundation Engineering, Hamburg, pp. 201–204.

Shogaki, T., 2006. An improved method for estimating *in-situ* undrained shear strength of natural deposits. Soils and Foundations 46 (2), 1–13.

Shogaki, T., Nakano, Y., Shibata, A., 2002. Sample recovery ratios and sampler penetration resistance in tube sampling for Niigata sand. Soils and Foundations 42 (5), 111–120.

Shogaki, T., Sakamoto, R., 2004. The applicability of a small diameter sampler with a two-chambered hydraulic piston for Japanese clay deposits. Soils and Foundations 44 (1), 113–124.

Shogaki, T., Ebisuzaki, D., Kanno, Y., Nakano, Y., Kitada, N., 2005. Geotechnical characteristics of Pisa clay. Tsuchi-to-kiso 53 (3), 27–29 (in Japanese).

Shogaki, T., Sakamato, S., Nakano, Y., Shibata, A., 2006. A applicability of the small diameter sampler for Niigata sand deposits. Soils and Foundations 46 (1), 1–14.

Shogaki, T., Kumagai, N., 2008. A slope stability analysis considering undrained strength anisotropy of natural clay deposits. Soils and Foundations 48 (6), 805–819.

Shogaki, T., Furukawa, T., Sato, M., Sugano, T., 2010. Applicability of estimating *in-situ* dynamic strength properties of Niigata sands. In: Proceedings of the 55th Geotechnical Symposium, pp. 213–220 (in Japanese).

Specifications for highway bridges, 2003. Japan Public Highway Corporation (in Japanese).

Suzuki, Y., Tokimatsu, K., Taya, Y., Kubota, Y., 1995. Relationship between CPT data, SPT data and liquefaction resistance of *in-situ* frozen samples. In: Proceedings of the 31st Annual Conference of JGS, pp. 983–984 (in Japanese).

Tatsuoka, F., Yasuda, S., Iwasaki, T., Tokida, K., 1980. Normalized dynamic undrained strength of sands subjected to cyclic and random loading. Soils and Foundations 20 (3), 1–14.

Tokimatsu, K., Yoshimi, Y., 1983. Empirical correlation of soil liquefaction based on SPT *N*-value and fines content. Soils and Foundations 23 (4), 56–74.

Tokimatsu, K., Uchida, A., 1990. Correlation between liquefaction resistance and shear wave velocity. Soils and Foundations 30 (2), 33–42.

Yoshimi, Y., Tokimatsu, K., Hosaka, Y., 1989. Evaluation of liquefaction resistance of clean sands based on high-quality undisturbed samples. Soils and Foundations 29 (1), 93–104.

Yoshimi, Y., 1994. Relationship among liquefaction resistance, SPT *N*-value and relative density for undisturbed samples of sands. Tsuchi-to-kiso 42 (4), 63–67 (in Japanese).